

Glass phase in anisotropic surface model for membranes

Hiroshi Koibuchi

Ibaraki National College of Technology, Nakane 866, Hitachinaka, Ibaraki 312-8508, Japan

E-mail: koibuchi@mech.ibaraki-ct.ac.jp

Andrey Shobukhov

Faculty of Computational Mathematics and Cybernetics, Lomonosov Moscow State University, 119991, Moscow, Leninskiye Gory, MSU, 2-nd Educational Building, Russia

Abstract. A Finsler geometric surface model for membranes is studied by using the Monte Carlo simulation technique on connection-fixed triangle lattices with sphere topology. An in-plane three-dimensional unit vector σ is assumed to be the in-plane tilt variable of the surface. The interaction with σ is described by the XY-model Hamiltonian. Since this variable σ is considered as a vector field on the surface, a Finsler metric is defined by using σ . We find that the model has three different phases. They change from the para-magnetic phase to the ferromagnetic and to the glass phases when the strength of the XY interaction increases. Both the para-magnetic and the glass phases are characterized by random configuration of σ ; the variable σ randomly fluctuates in the para-magnetic phase while it is randomly frozen in the glass phase. We also find that the surface becomes spherical in both phases. On the contrary, in the ferro-magnetic phase the surface shape becomes tubular or discotic due to the anisotropic bending rigidity and surface tension coefficient, which are dynamically generated by ordered configurations of σ .

1. Introduction

Anisotropic shape can be seen in biological membranes such as liposomes and vesicles [1] or in liquid crystal elastomers (LCEs) membranes [2, 3]. In those membranes, the strength of the surface force such as the surface tension γ and bending rigidity κ is expected to be dependent on whether these molecules are aligned or not. Indeed, the surface anisotropy can be obtained by modifying the bending rigidity κ to be dependent on the internal direction of surface in the Ginzburg-Landau or Helfrich-Polyakov (HP) model for membranes [4, 5]. However, the modification of κ in those models by hand gives only a constant κ over the surface although it should depend on the direction.

Another technique to make κ anisotropic is to assume a Finsler metric on the surface [6, 7]. In this approach, κ depends not only on the direction but also on the position on the surface. Since the Finsler geometric model is defined in a continuous form, its treatment such as the discretization is not always uniquely determined. In the anisotropic model of Ref. [6], we assumed that (i) the tilt variable σ belongs to \mathbf{S}^2 : unit sphere, and its tangential components are used as a vector field to define the Finsler metric, (ii) the Heisenberg spin model Hamiltonian S_0 is assumed for σ , (iii) the Finsler metric g_{ab}^F is constructed by deforming the Euclidean metric



δ_{ab} , (iv) g_{ab}^F is assumed for both the bond potential S_1 and the bending energy S_2 , while δ_{ab} is assumed for S_0 .

In this presentation, we show the results obtained for the model, which is different from the one in [6]. It is defined as follows: (i) $\sigma \in \mathbf{S}^1$: σ has the unit length, it belongs to the tangential plane and its values are assigned to the vertices, (ii) the XY model Hamiltonian S_0 is assumed for σ , (iii) g_{ab}^F is constructed by modifying the induced metric $g_{ab} = \partial_a X^\mu \partial_b X^\mu$, (iv) g_{ab}^F is assumed not only for S_1 and S_2 but also for S_0 .

2. Model

The model is defined on the triangulated surface in \mathbf{R}^3 , which is characterized by the three numbers (N, N_B, N_T) , which are the total numbers of vertices, bonds and triangles.

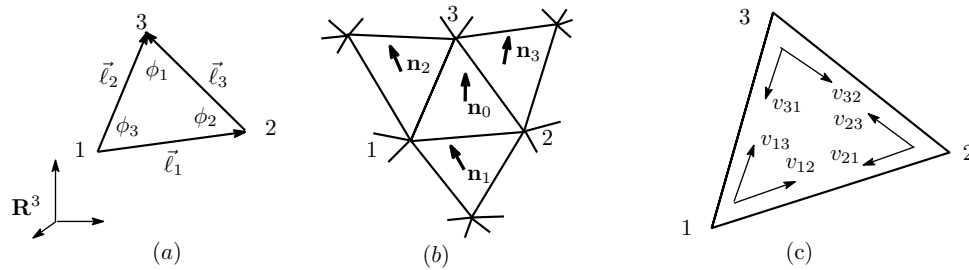


Figure 1. (a) Edge vectors $\vec{\ell}_i$ and internal angles ϕ_i of a triangle in \mathbf{R}^3 , (b) a triangle 123 and the three neighboring triangles, and (c) the parameters v_{ij} defined by Eq. (4).

The Hamiltonian is given by

$$S(X, \sigma) = \lambda S_0 + S_1 + \kappa S_2, \quad (1)$$

where S_0 is an energy for the directors (or tilts) σ_i . The σ_i has values in \mathbf{S}^1 , which is the unit circle on the tangential plane at the vertex i . The tangential plane is defined such that the unit normal vector $\hat{\mathbf{n}}_i$ at the vertex i is given by $\hat{\mathbf{n}}_i = \mathbf{N}_i / |\mathbf{N}_i|$, $\mathbf{N}_i = \sum_j \mathbf{n}_j a_j$, where \mathbf{n}_j and a_j are the unit normal vector and the area of the triangle j linked to the vertex i .

The internal energy S_0 , the Gaussian bond potential S_1 and the bending energy S_2 are defined as follows:

$$\begin{aligned} S_0 &= \frac{1}{6} \sum_{\Delta} S_{0\Delta} / a_{\Delta}, \quad S_1 = \frac{1}{6} \sum_{\Delta} S_{1\Delta} / a_{\Delta}, \quad S_2 = \frac{1}{6} \sum_{\Delta} S_{2\Delta} / a_{\Delta}, \\ S_{0\Delta} &= \left(v_{12} v_{13}^{-1} \ell_2^2 + v_{21} v_{23}^{-1} \ell_3^2 \right) (1 - \sigma_1 \cdot \sigma_2) + \left(v_{23} v_{21}^{-1} \ell_1^2 + v_{32} v_{31}^{-1} \ell_2^2 \right) (1 - \sigma_2 \cdot \sigma_3) \\ &\quad + \left(v_{13} v_{12}^{-1} \ell_1^2 + v_{31} v_{32}^{-1} \ell_3^2 \right) (1 - \sigma_3 \cdot \sigma_1) \\ &\quad - \vec{\ell}_1 \cdot \vec{\ell}_2 (\sigma_2 - \sigma_1) \cdot (\sigma_3 - \sigma_1) - \vec{\ell}_2 \cdot \vec{\ell}_3 (\sigma_1 - \sigma_3) \cdot (\sigma_2 - \sigma_3) \\ &\quad - \vec{\ell}_3 \cdot \vec{\ell}_1 (\sigma_3 - \sigma_2) \cdot (\sigma_1 - \sigma_2), \\ S_{1\Delta} &= \gamma_1 \ell_1^2 \ell_2^2 + \gamma_2 \ell_2^2 \ell_3^2 + \gamma_3 \ell_3^2 \ell_1^2 - 2 \left(\ell_1^2 \ell_2^2 \cos^2 \phi_3 + \ell_2^2 \ell_3^2 \cos^2 \phi_1 + \ell_3^2 \ell_1^2 \cos^2 \phi_2 \right), \quad (2) \\ S_{2\Delta} &= \kappa_1 \ell_1^2 (1 - \mathbf{n}_0 \cdot \mathbf{n}_1) + \kappa_2 \ell_2^2 (1 - \mathbf{n}_0 \cdot \mathbf{n}_2) + \kappa_3 \ell_3^2 (1 - \mathbf{n}_0 \cdot \mathbf{n}_3) \\ &\quad - \vec{\ell}_1 \cdot \vec{\ell}_2 (\mathbf{n}_0 - \mathbf{n}_1) \cdot (\mathbf{n}_0 - \mathbf{n}_2) - \vec{\ell}_2 \cdot \vec{\ell}_3 (\mathbf{n}_0 - \mathbf{n}_2) \cdot (\mathbf{n}_0 - \mathbf{n}_3) \\ &\quad - \vec{\ell}_3 \cdot \vec{\ell}_1 (\mathbf{n}_0 - \mathbf{n}_3) \cdot (\mathbf{n}_0 - \mathbf{n}_1), \end{aligned}$$

where $2 \cos^2 \phi_3$ in $S_{1\Delta}$ can also be written as $2 \cos^2 \phi_3 = (\ell_1^2 + \ell_2^2 - \ell_3^2) / \ell_1 \ell_2$. The symbols $\ell_i (i = 1, 2, 3)$ are the edge lengths of Δ , and $\mathbf{n}_i (i = 0, 1, 2, 3)$ denote the unit normal vectors of

triangles (Fig. 1(b)). The symbol a_Δ is the area of triangle Δ defined by $a_\Delta = (1/2)\ell_1\ell_2 \sin \phi_3 = (1/2)\ell_3\ell_1 \sin \phi_2 = (1/2)\ell_2\ell_3 \sin \phi_1$. The symbol \sum_Δ denotes the sum over all Δ . The coefficients γ_i and κ_i in Eq. (2) are defined by

$$\begin{aligned} \gamma_1 &= v_{13}v_{12}^{-1} + v_{12}v_{13}^{-1}, & \gamma_2 &= v_{32}v_{31}^{-1} + v_{31}v_{32}^{-1}, & \gamma_3 &= v_{21}v_{23}^{-1} + v_{23}v_{21}^{-1}, \\ \kappa_1 &= v_{13}v_{12}^{-1} + v_{23}v_{21}^{-1}, & \kappa_2 &= v_{12}v_{13}^{-1} + v_{32}v_{31}^{-1}, & \kappa_3 &= v_{21}v_{23}^{-1} + v_{31}v_{32}^{-1}. \end{aligned} \quad (3)$$

The parameters v_{ij} are given by

$$v_{ij} = 1 + [\sigma_{ij}], \quad \sigma_{ij} = N_v |\vec{\sigma}_i \cdot \mathbf{t}_{ij}|, \quad (4)$$

where $[x]$ represents $\text{Max}[n \in \mathbf{Z} | n \leq x]$, $N_v = 100$, and \mathbf{t}_{ij} is the unit tangential vector from the vertex i to the vertex j . The partition function Z is given by $Z(\lambda, \kappa) = \sum_\sigma \int' \prod_{i=1}^N dX_i \exp[-S(X, \sigma)]$, where $\int' \prod_{i=1}^N dX_i$ is the multiple three-dimensional integrations, that are performed by fixing the center of mass of the surface to the origin of \mathbf{R}^3 , and \sum_σ denotes the sum over tilt variables.

The assumed Finsler metric g_{ab}^F is given by $g_{ab}^F = \begin{pmatrix} \ell_1^2 v_{12}^{-2} & \vec{\ell}_1 \cdot \vec{\ell}_2 v_{12}^{-1} v_{13}^{-1} \\ \vec{\ell}_1 \cdot \vec{\ell}_2 v_{12}^{-1} v_{13}^{-1} & \ell_2^2 v_{13}^{-2} \end{pmatrix}$, which reduces to the discrete induced metric if $v_{ij} = 1$ for all ij . The discrete Hamiltonians S_0 , S_1 and S_2 in Eq. (2) with the coefficients in Eq. (3) are obtained from the continuous Hamiltonians just like in the model of Ref. [6].

3. Monte Carlo results

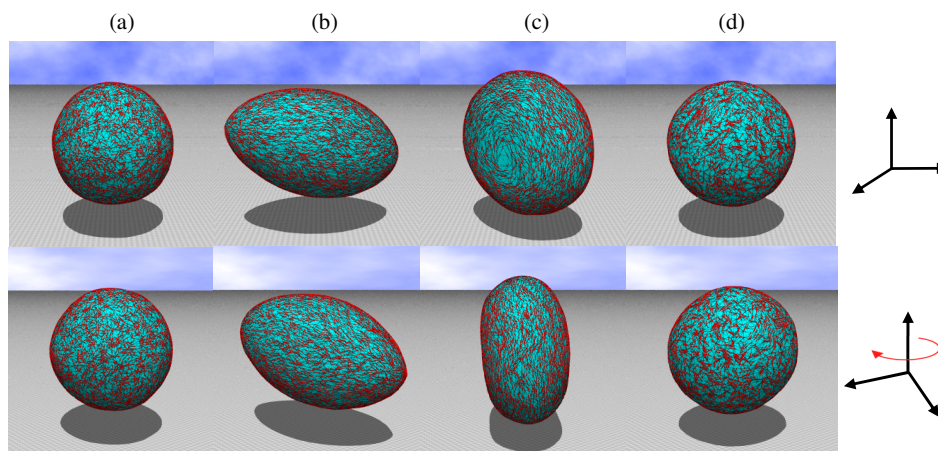


Figure 2. Snapshots for (a) $\lambda = 0.2$ (sphere), (b) $\lambda = 1.5$ (tube), (c) $\lambda = 3$ (disk), (d) $\lambda = 17$ (glass). $N = 5762$, $b = 300$, and $N_v = 100$. The view point of the lower snapshot is rotated about $\pi/4$ around the vertical axis of the upper one. Red brushes denote the in-plane variable σ .

We show snapshots for $\lambda = 0.2$, $\lambda = 1.5$, $\lambda = 3$, and $\lambda = 17$ (Figs.2(a)-2(d)), where the first one belongs to the high temperature phase and the remaining three belong to the low temperature phase. The random configurations in (a) and (d) correspond to the high temperature and the glass configurations, respectively. The magnetization M/N defined by $M/N = (1/N) |\sum_i \sigma_i| = (1/N) |(\sum_i \sigma_i^x, \sum_i \sigma_i^y, \sum_i \sigma_i^z)|$ reflects whether the spin variables *spatially* align or not (Fig. 3(a)). To the contrary, the following $[M]/N$ can reflect whether the spins *timely* align or not (Fig. 3(b)):

$$[M]/N = (1/N) \left| \sum_i M_i \right|, \quad M_i = \frac{1}{n_s} \left| \left(\sum_n \sigma_i^x(n), \sum_n \sigma_i^y(n), \sum_n \sigma_i^z(n) \right) \right| \quad (5)$$

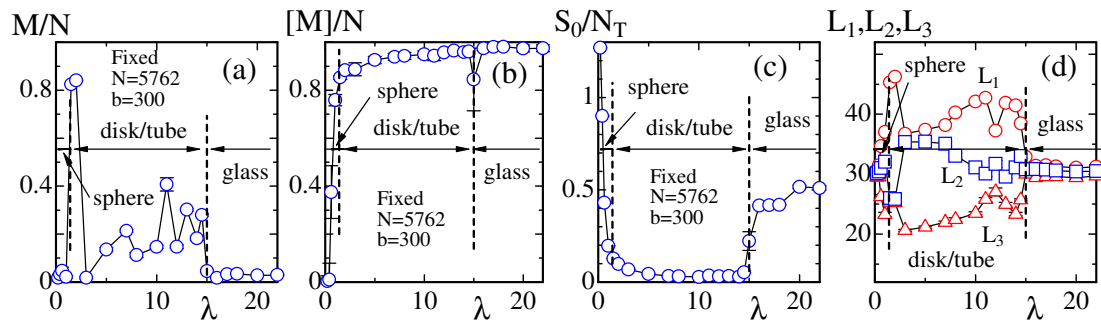


Figure 3. (a) M/N vs. λ , (b) $[M]/N$ vs. λ , (c) S_0/N_T vs. λ , and (d) L_i ($i=1, 2, 3$) vs. λ , where L_1 is the maximal linear extension and L_2, L_3 are diameters of the surface section perpendicular to the line from which L_1 is obtained.

where $n_s = \sum_n 1$ and $(1/n_s) \sum_n$ is the time series average of samples $\{\sigma_i(n)\}$, which is obtained at the vertex i with the Monte Carlo (MC) time n . The magnetization M/N is numerically obtained by performing the lattice average firstly and the time average finally, while $[M]/N$ is obtained with the time average firstly and with the lattice average finally. We expect $M/N \rightarrow 0$ if σ_i is spatially random, while $[M]/N \rightarrow 0$ if σ_i is timely random. Thus, the glass phase is characterized by $M/N \rightarrow 0$ and $[M]/N \rightarrow 1$. The glass phase is expected for $\lambda \geq 15$ (Figs. 3(a), (b)). In the high temperature phase, we see $M/N \rightarrow 0$ and $[M]/N \rightarrow 0$, which implies that σ is random both spatially and timely. In the low temperature phase for $\lambda \geq 1.5$, $[M]/N \rightarrow 1$ is expected because σ is timely unchanged or aligned whenever the surface is in the tube or disk configuration, while $M/N \rightarrow 1$ ($M/N \rightarrow 0$) is expected in the tube (disk) configuration.

At the phase boundary between the glass and disk/tube phases, S_0/N_T and the maximal (minimal) linear extension L_1 (L_3) appear to change discontinuously, where L_1 is the maximal surface length along the line going through the center of surface, while L_2 is the maximal diameter of the sectional ellipse which is perpendicular to the line corresponding to L_1 , and L_3 is the ellipse diameter at the line vertical to both of the lines corresponding to L_1 and L_2 . We see $L_1 \simeq L_2 \simeq L_3$ in the glass phase (Fig. 3(d)), which implies that the surface is spherical in this phase. The surface shape in the disk/tube phase seems to be dependent on the initial condition in contrast to the model in Ref. [6].

The glass phase of the model is expected to be not stable but quasi-stable. Indeed, the mean field analysis of the Finsler XY model defined by $S = \lambda S_0$ with $\ell_i = 1$ on the regular square lattice indicates that the free energy has a quasi-stable state corresponding to the glass phase. This will be reported elsewhere. The author (HK) acknowledges Hideo Sekino in Toyohashi University of Technology for comments.

References

- [1] H.-G. Döbereiner and U. Seifert, *Europhys. Lett.* **36**, 325 (1996).
- [2] Xiangjun Xing, Ranjan Mukhopadhyay, T. C. Lubensky, and Leo Radzihovsky, *Phys. Rev. E.* **68** (2003) 021108(1-17).
- [3] Xiangjun Xing and Leo Radzihovsky, *Annals of Phys.* **323** (2008) 105.
- [4] L. Radzihovsky, in *Statistical Mechanics of Membranes and Surfaces*, Second Edition, edited by D. Nelson, T. Piran, and S. Weinberg, (World Scientific, 2004) p.275.
- [5] M. Bowick and A. Travesset, *Phys. Rep.* **344** (2001) 255.
- [6] H. Koibuchi "A Finsler geometric model for membranes on triangulated surfaces", ic-msquare2102, *Journal of Physics Conference Series* Vol. 410 (2013) 012056 (4 pages).
- [7] H. Koibuchi and H. Sekino, "Monte Carlo studies of a Finsler geometric surface model", *Physica A* (in press), <http://arxiv.org/abs/1208.1806>.